

An Atlas of Monte Carlo Models of Dust Extinction in Galaxies for Cosmological Applications

Andrea Ferrara¹, Simone Bianchi², Andrea Cimatti¹ and Carlo Giovanardi¹

¹Osservatorio Astrofisico di Arcetri

50125 Firenze, Italy

E-mail: ferrara@arcetri.astro.it

E-mail: cimatti@arcetri.astro.it

E-mail: giova@arcetri.astro.it

²Dept. of Physics and Astronomy, University of Wales Cardiff

P.O. Box 913, Cardiff Wales, CF2 3YB, UK

E-mail: Simone.Bianchi@astro.cf.ac.uk

Received _____; accepted _____

ABSTRACT

We present an extensive study of the radiative transfer in dusty galaxies based on Monte Carlo simulations. The main output of these simulations are the attenuation curves \mathcal{A}_λ (*i.e.* the ratio between the observed, dust extinguished, total intensity to the intrinsic unextinguished one of the galaxy as a function of wavelength). We have explored the dependence of \mathcal{A}_λ on a conspicuous set of quantities (Hubble type, inclination, dust optical thickness, dust distribution and extinction properties) for a large wavelength interval, ranging from 1250Å to the K band, thus finally providing a comprehensive atlas of dust extinction in galaxies, which is electronically available. This study is particularly suitable for inclusion into galaxy formation evolution models and to directly interpret observational data on high redshift galaxies.

Subject headings: dust, extinction – galaxies: ISM – galaxies: evolution – radiative transfer

1. Motivation

Modelling galaxy formation at high redshift, both via semi-analytical methods and numerical simulations, has become one of the most active areas in cosmology in the last decade. As the observational identification of galaxies is proceeding very rapidly to high redshift (the present record being held by a galaxy at redshift $z = 5.60$, Spinrad *et al.* 1998) thanks to the well-established Lyman-dropout technique (Steidel *et al.* 1996, Madau *et al.* 1996), a considerable effort has to be devoted to the development of models of increasing complexity, necessary to interpret the observed properties of such objects. The detection of distant galaxies made possible by recent UV/visible surveys has allowed investigators to tackle the problem of the global star formation rate in the universe (SFR) in a quantitative manner. We have now clarified that stars were forming at $z \approx 1$ at a rate about ten times higher than at present. During this period, the forming galaxies have converted a considerable fraction of baryons into stars, an effect that is likely seen in the decrease of the cold gas comoving density between $z = 2$ and $z = 0$. The evolution of the SFR at even higher redshift is, however, not yet fully established. The main difficulty to this concern is the fact that approaches based on the dropout technique are poorly sensitive to dust-obscured galaxies. Hence, the SFR deduced in this way could represent a severe underestimate of the actual one, if even a rather modest amount of dust is present in the interstellar medium of the star forming galaxy. Also, some galaxies could be so heavily extinguished that they could be completely missed from the UV/visible census. Support to this possibility is lent by available IR (Rowan-Robinson *et al.* 1997) and sub-mm (Smail *et al.* 1997, Cimatti *et al.* 1998) observations that have explicitly tackled this problem. Using the modelled SED of 12 galaxies detected by ISO in the HDF, Smail *et al.* derived star formation rates significantly higher than those derived by Madau *et al.* (1996). From the analysis of source counts at two wavelengths (450 and 850 μm) in a survey exploiting the high sensitivity SCUBA bolometer array, these authors also concluded that the number

density of star forming galaxies strongly increases in the high redshift universe. These results are further substantiated by the similar conclusions reached by Franceschini *et al.* 1997, who studied K-band selected early type galaxies in the HDF, and by statistical approaches as those in Pozzetti *et al.* 1998.

At present, probably the most successful class of models developed to study the formation and evolution of galaxies are based on the hierarchical paradigm, *i.e.* structure in the universe grows by association of small units to form larger bound objects. Starting from a number of (more or less heuristic) prescriptions ruling the gas collapse in the dark matter halos, the process of star formation, stellar feedback and evolution, these models are able to predict several observables characterizing real galaxies. This approach has been refined to an increasing degree of sophistication and applied to different aspects by a large number of groups (White & Frenk 1991, Lacey *et al.* 1993, Kauffman 1995, Ciardi & Ferrara 1997, Baugh *et al.* 1997, Guiderdoni *et al.* 1998). However, at least one aspect of this type of studies – dust effects – has probably been overlooked or at best only very coarsely treated. An effort is therefore required to include a proper dust treatment not only in these semi-analytical type of models, but also in extensive numerical simulations and even in more direct data interpretations. Typically, such studies make very simple (and sometimes crude) approximations about the dust component of galaxies. A standard set would, for example, assume that (i) the dust is distributed as the stars, (ii) inclination-dependent extinction effects can be averaged, (iii) the scattering of grains is often assumed as isotropic and the albedo treated in a heuristic way, and finally (iv) "screen" or "sandwich" geometries are adopted, in which there is a layer of pure dust between the observer and any stars. In addition, physical effects related to the different optical thickness of protogalaxies (which according to the above discussion could be substantial) and to the possibly different extinction curve remain largely to be explored. The assumption of "screen" geometries, resulting in a more efficient extinction of galactic light with respect to distributions with

the dust and stars mixed, typically tends to underestimate the amount of dust. This effect is confirmed by comparison with FIR/sub-mm observations, which are sensitive to dust thermal emission, which often yield dust masses larger than expected on the basis of screen geometry absorption estimates. Using realistic dust distributions and detailed radiative transfer helps reconcile the above discrepancy. For example, our mass estimate for the red galaxy HR10 (Cimatti *et al.* 1997) using Monte Carlo simulations of the type presented here is in close agreement with the one obtained from sub-mm data (Cimatti *et al.* 1998). The ongoing work by Cole *et al.* (1998), which is using some of the present results, and the recent study by Silva *et al.* (1998) modelling the effects of dust on galactic SEDs, very likely are setting the scene for additional progress in this area.

Only recently more realistic models have been developed (Kylafis & Bahcall 1987; Bruzual *et al.* 1988; Witt *et al.* 1992; Byun *et al.* 1994; Wise & Silva 1996; Bianchi, Ferrara & Giovanardi 1996, hereafter BFG). Although these models have shown that dust scattering plays an important role by reducing the effects of dust absorption, no systematic studies of the effects of the extinction on the observed colours of high- z galaxies have been performed. Understanding these effects is crucial in cosmology and galaxy evolution studies.

The main aim of this work is to provide a large database of dust extinction cases that could be safely included into galaxy evolution models, numerical simulations, and interpretation of observational results. The way in which we accomplish this task is by using the Monte Carlo numerical code originally developed to simulate the extinction and polarization properties of spiral galaxies (described in Bianchi, Ferrara & Giovanardi 1996). The code has been adapted to include a number of aspects discussed below, and to obtain handy and directly relevant quantities as the attenuation curves \mathcal{A}_λ (*i.e.* the ratio between the observed, dust extinguished, total intensity to the intrinsic unextinguished one of the galaxy as a function of wavelength). We have explored the dependence of \mathcal{A}_λ on a set of

observable quantities (Hubble type, inclination, dust optical thickness, dust distribution and extinction properties) for a large wavelength interval, ranging from the 1250Å to the K band, thus finally providing a comprehensive atlas of dust extinction in galaxies. This study could be used in the future for a number of different applications; as an example, Cimatti *et al.* (1997) have exploited some of the results presented here to investigate the problem of the age-dust degeneracy in high- z elliptical galaxies.

The plan of the paper is the following. In § 2 we present in detail our dusty galaxy models, emphasizing the changes with respect to BFG, and the model classification adopted; § 3 is devoted to the results, mainly constituted by the attenuation curves for the various cases (obviously, due to the huge amount of data only a small subset are shown here, but attenuation curves for all the studied cases are available in electronic form – see § 5). Finally, § 4 contains a few additional comments concerning the general applicability of our results.

2. Dusty Galaxy Models

In order to study the effects of dust extinction, a realistic model for the light and dust distribution in galaxies is required. We start by dividing galaxies in two broad classes according to their stellar distribution: spirals and ellipticals, respectively. The former are characterized by a disk and a bulge, whereas ellipticals consist of a bulge only.

For both types of galaxies we consider two different dust extinction curves, reproducing the results for the (i) Milky Way (MW) and (ii) the Small Magellanic Cloud (SMC) (Gordon *et al.* 1997). The adopted curves are shown in Fig. 1. The main difference between them is the relevance of the 2175Å bump, absent in the SMC extinction law. The physical interpretation of such a feature in terms of the type, shape and eventually coating

of the grains producing it remains still unclear (for a discussion see, for example, Draine & Malhotra 1993). The common wisdom is to assume that in starburst galaxies the bump is weak or absent. This idea is based on observations of the extinction curve in the 30 Dor region, (often considered as a starburst prototype) showing that the feature is very weak, whereas outside the region the extinction curve is similar to the Galactic one (Fitzpatrick 1985, 1986). The bump has been recently detected also in high redshift Mg II absorbers (Malhotra 1997), thus suggesting that the dust properties in the young universe could be rather similar to the local ones. Finally, one has to keep in mind that the absence of this extinction feature in external galaxies could be due either to a different dust composition or to scattering effects compensating for dust absorption, as shown by Cimatti *et al.* (1997).

We explore several possible distributions of galactic dust in order to cover a wide range of possible applications, which are described in detail below. For each distribution we have studied 9 values of the optical depth in the V-band ($\tau_V = 0, 0.1, 0.5, 1, 2, 5, 10, 20, 50$) in the rest frame of the galaxy along a line of sight passing through the center of the galaxy (perpendicular to the galactic plane, when a dust disk is present). The total galactic dust mass can be calculated from a given value of τ_V by using the conversion formulae given in Appendix A, which depend on grain properties and dust distribution.

2.1. Spiral Galaxies

2.1.1. Stellar Distribution

Following BFG, we describe the stellar spatial distribution in spirals by two components: a spheroidal bulge and a three-dimensional disk. We neglect dark, massive halos, since we are interested only in luminous components, and possible small scale inhomogeneities, such as spiral arms and/or star-forming regions.

Disk The stellar disk luminosity density is supposed to be appropriately described by an exponential distribution, both horizontally and vertically. The horizontal scale length is $r_\star = 4$ kpc; the vertical scale height is $z_\star = 0.35$ kpc; these parameters are fixed to match the observed values for the old disk population of the Galaxy. The disk is horizontally and vertically truncated at a distance r_{max} equal to 6 times the corresponding scale length.

Bulge The luminosity density distribution of this component is modelled as a Jaffe bulge (see BFG) which reproduces the $r^{1/4}$ profile characteristic of elliptical and bulge systems. We adopt an effective radius proportional to the scale length of the disk, $r_e = \eta r_\star$ with the constant η allowed to take the following three values: $\eta = 0.1, 0.4, 1.6$. The bulge is truncated at a distance equal to $r_{max} = 5r_e$.

B/T and Inclination To simulate different Hubble types, we consider different bulge-to-total luminosity ratios. Specifically, we study the cases B/T=0, 0.1, 0.3, 0.5, 1. which should approximate the entire Hubble sequence from Sd to Sa types, respectively. The simulated galaxy is observed in 9 different inclination bands, centered on the angles: $i = 9.31^\circ, 22.9^\circ, 30^\circ, 40^\circ, 50^\circ, 60^\circ, 70^\circ, 80^\circ, 90^\circ$ (edge on). Edge-on images contains all the photons between 88.5° and 91.5° . The width of each inclination band is set to cover the same solid angle as the edge-on case (see BFG).

2.1.2. Dust Distribution

Disk The dust is assumed to be smoothly distributed in the same plane as the stellar disk and with a double exponential distribution as the stellar one. The horizontal scale length is the same as for the stars, $r_d = r_\star = 4$ kpc; the vertical scale height is instead $z_d = \xi z_\star$, with $\xi = 0.4, 1., 2.5$, thus simulating dust that is less or more extended than the stars, respectively.

Motivated by the recent suggestions that dust can be not only vertically but also horizontally more extended than stars (Ferrara *et al.* 1991, Ferrara 1997, Davies *et al.* 1997, Xilouris *et al.* 1997, 1998), we have also studied a particular case identified by $r_d = 1.5r_*$, $\xi = 2$ and $\eta = 0.4$. This case should suitably incorporate the recent findings by Davies *et al.* (1997) on the Galaxy.

2.1.3. Model Classification

The spiral galaxy models can be classified according to this system. The first letter is a S for "spiral"; the 2nd and 3th character refer to the value of η corresponding to the given model. An underscore introduces the part of the word referring to the dust properties: the adopted extinction curve (M=Milky Way, S=Small Magellanic Cloud), E stands for double "Exponential" distribution (one case is labelled "D" and refers to the radially extended dust distribution suggested by Davies *et al.* 1997). Finally, the remaining two characters give the value of ξ . Thus, for example, the model S01_ME04 identifies the spiral galaxy model with $\eta = 0.1$ with Milky Way-type dust distributed according to a double exponential law, whose scale height is $\xi = 0.4$ times smaller than the stellar scale height. For each of these models the entire set of B/T, inclination and τ_V values given above has to be simulated. A summary of the model properties is given again in Tab. 1.

2.2. Elliptical Galaxies

2.2.1. Stellar Distribution

We describe the stellar luminosity density distribution of elliptical galaxies with a Jaffe bulge. We adopt a fixed effective radius $r_e = 4$ kpc truncated at $r_{max} = 5r_e = 20$ kpc. Thus, elliptical galaxies in our scheme have only the single value B/T=1; also, for models

in which the dust is spherically distributed, given the complete spherical symmetry of the system, it is obviously not necessary to simulate different inclinations.

2.2.2. Dust Distribution

For elliptical galaxies we investigate the effects of the four different dust distributions described in the following.

Model E Dust is distributed in a double exponential disk, similarly to the spiral galaxy case, with $r_d = 4$ kpc and $z_d = 0.05$ kpc (Cimatti *et al.* 1997). Inclinations are the same as in that case as well, $i = 9.31^\circ, 22.9^\circ, 30^\circ, 40^\circ, 50^\circ, 60^\circ, 70^\circ, 80^\circ, 90^\circ$ (edge on).

Model C Dust has a constant density inside a sphere with the same radius as the bulge, $r_{max} = 5r_e = 20$ kpc.

Model J This model assumes that the dust is distributed as the light, *i.e.* with a Jaffe density distribution having the same parameters as the bulge: $r_e = 4$ kpc, $r_{max} = 5r_e = 20$ kpc. As the density in a Jaffe bulge diverges at $r = 0$, we have defined τ_V along a line of sight passing through $r = r_e$ for this model.

Model R Finally we have considered a model in which the dust density profile decreases as r^{-1} out to a radius $r_{max} = 20$ kpc. In analogy with model J, the central divergence of the adopted profile, forces us to define τ_V along a line of sight passing through a radius $r_o = 15.7$ kpc which contains the same dust fraction (61.6%) inside r_e in our Jaffe distribution.

2.2.3. Model Classification

In analogy with spiral galaxies, we introduce a classification scheme for elliptical galaxies as well. In this case, the first letter is a E for "elliptical". As the stellar component has fixed parameters, no other information about the light distribution is needed. Again, the underscore introduces the part of the string referring to dust properties: the first character after the underscore denotes the type of extinction curve (M=Milky Way, S=Small Magellanic Cloud). The next (and final) character identifies one of the four studied dust distributions. Using the nomenclature already introduced in the previous section, we use "E" for double exponential, "C" for a constant density sphere, "J" for a Jaffe spherical distribution, and "R" for a r^{-1} spherical distribution. Thus, for example, the model E_ME identifies the elliptical galaxy model with with Milky Way-type dust distributed according to a double exponential law, with parameters defined above. For E_ME and E_SE models all the inclination and τ_V values given above have to be simulated; as models "C", "J", and "R" are spherically symmetric, only runs for the 9 adopted values of τ_V are calculated. A summary of the model properties is given in Tab. 1.

3. Attenuation Curves from Monte Carlo Simulations

In order to calculate the attenuation properties of the various models of spiral and elliptical galaxies, we have performed a large number of Monte Carlo simulations. These simulations allow us to treat the radiative transfer in dusty galaxies (*i.e.* considering the extinction as the combination of absorption and scattering). The Monte Carlo code that we use for this study is adapted from the one already presented in BFG and we defer the interested reader to that paper for details. The difference consists in the fact that in this work we consider a simplified single grain approach, with a Henyey-Greenstein scattering phase function (Henyey & Greenstein 1941; see also BFG): scattering properties are thus

defined by a single value of the albedo ω and of the asymmetry parameter g . Values of ω and g are taken from Gordon *et al.* (1997). The polarization part in the radiative transfer code has been omitted.

The main output from the Monte Carlo simulations are the attenuation curves \mathcal{A}_λ . These are defined as

$$\mathcal{A}_\lambda = \frac{\text{Observed, dust extinguished, total intensity } I_{obs}(\lambda)}{\text{Intrinsic, unextinguished, total intensity } I_0(\lambda)} \quad (1)$$

In general, \mathcal{A}_λ is a function of τ_V , i and B/T. The attenuation curves are calculated for 14 wavelength bands defined in Gordon *et al.* 1997: UV1, UV2, UV3, UV4, UV5, UV6, UV7, U, B, V, R, I, J, K, with central wavelength $\lambda = 1250, 1515, 1775, 1995, 2215, 2480, 2895, 3605, 4413, 5512, 6594, 8059, 12369, 21578$ Å, respectively. As an example of the data (available in electronic form at the web site <http://www.arcetri.astro.it/~sbianchi/attenuation.html>) we show attenuation curves for some cases selected from four representative models (summarized in Tab. 1) in Figs. 2-3. In addition, Fig. 4 shows the wavelength dependence of the fraction of the emitted energy absorbed by dust for a spiral galaxy model. This quantity could be used together with the observed stellar SED and FIR luminosity, to retrieve the intrinsic *unextinguished* stellar emission. In models with spherical symmetry both for stars and dust (*e.g.* E_xC, E_xJ, E_xR), the fraction of emitted energy absorbed by dust is simply $1 - \mathcal{A}_\lambda$. These data are also available in electronic form at the above site.

3.1. Trends in the Attenuation Curves

We give now a general description of the attenuation curves aimed at isolating the effects of the various galactic and dust properties investigated.

a) Wavelength dependence

The \mathcal{A}_λ curves in all cases show an overall increasing trend as a function of the

observed wavelength λ ; this closely reflects the behaviour of the extinction curves. When the 2200Å bump is present in the extinction curve (*i.e.* MW-type), its footprint is also seen in the attenuation curves, although with varying strength, which depends on inclination and optical depth. This effect is explained by scattering modulation due to geometry and multiple scattering of photons on dust grains, respectively.

b) Hubble Type dependence

The main difference between the pure disk (B/T=0) and bulge (B/T=1) cases is that disks are more absorbed at high inclinations (*i.e.* edge-on) because of the larger optical depth of the dust in the plane of the galaxy. Bulges, instead, are more attenuated at low i , as in that case basically only the foreground part of the spheroid is seen, whereas as i is increased almost the entire bulge comes into view, provided the dust thickness is not substantial with respect to the bulge effective radius. This case implies large η and low ξ values.

c) Dust Optical Depth and Distribution

The behaviour of \mathcal{A}_λ with the dust optical depth τ_V is rather straightforward to interpret: more light is absorbed by increasing τ_V although in some cases saturation at $\tau_V \gtrsim 5$ occurs, particularly in UV/optical bands. The effect of increasing η , *i.e.* more extended bulges, typically causes, for a given value of τ_V and i , the galaxy to be less attenuated. This is due to the fact that a larger fraction of the bulge emitted light is outside the dust obscuring layer. The amount of attenuation decreases as i is increased, both for disk- and bulge-dominated galaxies. However, there are exceptions to this rule for early Hubble types, where the bulge is particularly pronounced (*e.g.* S16_ME04 model) or small compared to the dust scale height (*e.g.* S01_ME25): in the first case more edge-on galaxies allow for a larger fraction of the galactic bulge light to escape freely; in the second case, inclination effects are basically negligible as the bulge is only seen through the dust layer at

any inclination to the line of sight.

The thickness of the dust layer, described by the parameter ξ profoundly affects the observable spectral energy distribution of the galaxy. An increase of a factor 2.5 in the value of ξ typically causes a drop in \mathcal{A}_λ by ≈ 0.1 at UV/optical wavelengths, whereas the change in the near IR (J and K bands) is much smaller. For large values of $\xi = 2.5$, and of the optical depth, only a fraction $\lesssim 1\%$ of the emitted photons can escape from the galaxy (see model S01_ME25). This effect is particularly evident for small bulges, which therefore can be almost totally obscured in the UV/optical bands even at relatively low τ_V , a fact that can have important consequences, as mentioned in § 1.

The class of models implementing horizontally extended dust distributions (S04_MD20 and S04_SD20) are much more extinguished than other models with comparable vertical dust scale height. Disk-dominated galaxies are obviously more sensitive to this different dust distribution than bulge-dominated objects, as stars are intermixed with sufficiently optically thick dust in a larger area of the disk.

d) Extinction Curves

Different extinction curves do not seem to produce relevant qualitative differences, apart from the presence/absence of the 2200Å bump in the attenuation curves. Quantitative differences are restricted to a few percent level.

e) Elliptical Galaxies

Finally, among the models investigated for elliptical galaxies the exponential dust distribution (model E_ME) produces the smallest attenuation factors (in this case the dust disk scale height is relatively thin, $z_d = 50$ pc). Among the spherically symmetric models, the constant (E_MC), and $1/r$ (E_MR) distributions give similar results being able to efficiently attenuate the most luminous central regions of the bulge. For the Jaffe distribution, in which the dust is well intermixed with the stars, the attenuation is

considerably reduced with respect to the other two above cases.

4. An Application to Local Spirals

The models presented above are particularly suitable to study the effects of dust in distant galaxies, for which only integral properties as, for example, the total apparent magnitude in a given band is known.

Nevertheless, testing our predictions against local observational data allows to calibrate our models to the nearby universe. In addition, the derived galactic properties (*e.g.* dust optical depth, geometry, etc) might serve as a guide when exploring their counterparts in the young universe.

As an example, in the following we study the dependence of the total apparent magnitude m of a galaxy in a given band on the inclination angle i . Obviously, in the absence of dust, there would be no reason to expect a correlation between these two quantities in a sample of galaxies of the same mass, as from the Tully-Fisher relation it follows that they should consequently have the same luminosity. The inclination dependence of apparent magnitudes is instead now well established (de Vaucouleurs *et al.* 1991, Giovanelli *et al.* 1994, Peletier & Willner 1992, Peletier *et al.* 1994, Evans 1994, Bernstein *et al.* 1994) and thought to depend on dust obscuring effects. This internal attenuation results in a magnitude correction Δm which is inclination-dependent, in the sense that more edge-on galaxies appear fainter. In Fig. 5 we compare the predicted values $\Delta m = -2.5 \log \mathcal{A}_\lambda$ with the fit to the observational values derived by de Vaucouleurs *et al.* (1991) [$\Delta m = 1.45 \log(1/\cos i)$] in the B-band, and by Bernstein *et al.* (1994) [$\Delta m = 1.4(1 - \cos i)$] in the I-band. As both samples mostly contain Sb-Sd galaxies, we choose B/T=0.1 models, MW-type extinction, and use the value $\eta = 0.4$ appropriate

for the Milky Way (see BFG); this defines the class of models S04_ME xx . For each band we compare the data with Δm curves as a function of $1 - \cos i$ for three values of $\xi = 0.4, 1.0, 2.5$ and 4 values of $\tau_V = 0.5, 1, 5, 10$. The abscissa limits are dictated by the availability of data for different inclinations. The conclusion from the inspection of Fig. 5 is rather straightforward: only models which assume a central $\tau_V \sim 5 - 10$ can simultaneously fit the data in both bands; also, models in which the dust thickness is larger (higher ξ) seem to perform better. Note that the vertical offset between the data points and the curves (they have been normalized at the same value at $i = 60^\circ$ or $(1 - \cos i) = 0.5$) is arbitrary as the dust-free luminosity cannot be experimentally determined. This simple example shows how our models are able to satisfactorily reproduce the high quality data available locally; therefore, unless the properties of dust and galaxies are considerably different in the young universe, the hope is that they could serve to robustly model the effects of dust at high redshift as well.

5. Clumping effects

As a final remark, we like to recall that our models do not include yet the possible existence of a clumpy dust component in addition to the smoothly distributed one considered. The extension of the present work to such a case is already in progress; here we would like to discuss briefly the consequences of our smooth distribution assumption deduced from these preliminary results.

High redshift galaxies often show rather irregular morphologies suggestive of inhomogeneous dust and light distribution (Abraham *et al.* 1996), possibly produced by the higher merging/interaction rates at those epochs. On the other hand, Giavalisco *et al.* 1996 found that UV dropouts at $z > 3$ either show a core similar to present day spheroids or are described by exponential luminosity profiles, thus providing a solid observational basis for

our assumptions.

As a general rule, clumpiness typically results in a lower effective dust optical depth and may affect the wavelength dependence of the attenuation curves. Estimating by how much our models might be overestimating the attenuation is not trivial as, if we allow for the dust to partly reside in clumps, at least three additional parameters should be introduced. These are: the clump/interclump dust density contrast, the size of the clumps and the filling factor of clumps. The above parameters are only loosely constrained by current observations. The mere schematization of the dust distribution as a two-component medium made of clumps and interclump medium escapes a clear physical interpretation, as several possibilities arise from the complexity of the ISM: (i) can the dust clumps be identified with molecular clouds ? In this case they should be distributed in the galaxy following the molecular hydrogen abundance, rather than randomly; (ii) are they the so-called "clumpuscles" proposed by several authors as dark matter candidates ? if so, their sizes and masses should be pretty small (30 AU and Jupiter mass, respectively; Pfenninger & Combes 1994); (iii) do they arise in fractal-like density fluctuations in the ISM ? A spectrum of sizes should be then expected and the modelling would become computationally quite expensive; finally, (iv) are they a reflection of transient coherent features as dust lanes or produced by dynamical effects as galaxy interactions, merging, stripping or spiral density waves ? It is clear that the very nature of these clumps strongly affects that way in which we include clumpiness in the models or we interpret its observational consequences. A lot of effort to understand these issues from the experimental point of view is necessary to make a progress. Even if the value of the free parameters would be perfectly known, the only way to assess their effects would be to perform Monte Carlo simulations of the type presented in this paper. Our preliminary runs including a clumpy component modelled as spherical clouds of different size and number, suggest that the attenuation curves start to become insensitive to presence of inhomogeneities above a critical inclination angle $i_c(f)$ which depends on the

value of the clump filling factor f . Already for $f \approx 0.2$ the critical inclination approaches values as low as $i_c = 40^\circ$; for higher values of f the differences in the attenuation curves are almost unnoticed. This conclusion, although preliminary, seems to be in agreement with the findings of recent/ongoing work by different groups (Byun & Lee 1997, Kuchinski *et al.* 1998). If confirmed, these arguments imply that the effect of clumping is much less dramatic than usually believed, although further study - both theoretical and observational - is clearly needed.

6. Attachments

The electronic source files containing the attenuation (of the type shown in Figs. 2-3) and energy absorption (Fig. 4) curves for the entire set of models described here and summarized in Tab. 1, can be retrieved from the web site <http://www.arcetri.astro.it/~sbianchi/attenuation.html>.

We thank C. Lacey for stimulating discussions and for suggesting the comparison with local galaxies and the referee, J. Mathis, for very insightful and useful comments.

7. Appendix A

In the following we give the formulae allowing to convert the value of the optical thickness τ_V into a total galactic dust mass for the four dust distributions considered in this paper, with the assumptions for the average grain radius, a , V-band extinction coefficient, Q , and grain density, δ given below.

$$a = 0.1\mu \text{ m, average grain radius}$$

$$Q = 1.5, \text{ V - band extinction coefficient}$$

$$\delta = 2 \text{ g cm}^{-3} \text{ grain density}$$

exponential disk

$$M = \tau_V \alpha_d^2 \frac{8\pi a\delta}{3 Q} \left[1 - (n+1)e^{-n} \right] \quad (n = 6 \text{ truncation factor})$$

$$M [M_\odot] = 5.3 \times 10^5 \tau_V (\alpha_d [\text{kpc}])^2$$

$$M [M_\odot] = 8.4 \times 10^6 \tau_V \quad \alpha_d = 4 \text{ kpc}$$

$$M [M_\odot] = 1.9 \times 10^7 \tau_V \quad \alpha_d = 6 \text{ kpc}$$

constant sphere

$$M = \tau_V r_{max}^2 \frac{8\pi a\delta}{9 Q}$$

$$M [M_\odot] = 1.8 \times 10^5 \tau_V (r_{max} [\text{kpc}])^2$$

$$M [M_\odot] = 7.1 \times 10^7 \tau_V \quad r_{max} = 20 \text{ kpc}$$

Jaffe sphere

$$M = \tau_V r_0^2 \frac{8\pi}{3} \frac{a\delta}{Q} \left[\frac{\frac{n}{n+1}}{\text{asin}(1) - \text{asin}(1/n) - \frac{\sqrt{n^2-1}(5+4n)}{3(1+n)^2}} \right]$$

$$r_0 = 4.64 \text{ kpc} \quad (\text{corresponding to } r_e = 4 \text{ kpc}) \quad r_{max} = 20 \text{ kpc} \quad n = r_{max}/r_0$$

$$M [M_\odot] = 1.8 \times 10^6 \tau_V r_0^2$$

$$M [M_\odot] = 4.0 \times 10^7 \tau_V$$

1/r sphere

$$M = \tau_V r_0^2 \frac{4\pi}{3} \frac{a\delta}{Q} \left[\frac{n^2}{\ln(n + \sqrt{n^2-1})} \right]$$

$$r_0 = 15.7 \text{ kpc} \quad r_{max} = 20 \text{ kpc} \quad n = r_{max}/r_0$$

$$M [M_\odot] = 6.0 \times 10^5 \tau_V r_0^2$$

$$M [M_\odot] = 1.5 \times 10^8 \tau_V$$

REFERENCES

- Abraham, R. G., Tanvir, N. R., Santiago, B. X., Ellis, R. S., Glazebrook, K. & Van den Bergh, S. 1996, MNRAS, 279, 47
- Baugh, C. M., Cole, S., Frenk, C. S., & Lacey, C. G. 1997, preprint (astro-ph/9703111)
- Bernstein, G. M. *et al.* , 1994, AJ, 107, 1962
- Bianchi, S., Ferrara, A. & Giovanardi, C. 1996, ApJ, 465, 127 (BFG)
- Bruzual, G., Magris G. & Calvet, N. 1988, ApJ, 333, 673
- Byun, Y. I., Freeman, K. C., & Kylafis, N. D. 1994, ApJ, 432, 114 Byun, Y. & Lee, T. 1997, BAAS, 191, 7503
- Cimatti, A., Bianchi, S., Ferrara, A. & Giovanardi, C. 1997, MNRAS, 290, L43
- Cimatti, A., Andreani, P., Röttgering, H., Tilanus R. 1998, Nature, 392, 895
- Cole, S., Lacey, C. G. Frenk, C. S. & Baugh, C. M. 1998, in preparation
- Ciardi, B., & Ferrara, A. 1997, ApJL, 483, 5
- Davies, J. I., Trewhella, M., Jones, H., Lisk, C., Madden, A., & Moss, J. 1997, MNRAS, 288, 679
- de Vaucouleurs, G., de Vaucouleurs, A., Corwin, H. G., Buta, R. J., Pature, G. & Forqué, P. 1991, Third References Catalogue of Bright Galaxies (New York: Springer)
- Draine, B. T. & Malhotra, S. 1993, ApJ, 414, 632
- Evans, R. 1994, MNRAS, 266, 511
- Ferrara, A., Ferrini, F., Franco, J., & Barsella, B. 1991, ApJ, 381, 137
- Ferrara, A. 1997, “The Physics of Galactic Halos”, 156th WE-Heraeus-Seminar, eds. Lesch *et al.* , (Verlag: Berlin), 189
- Fitzpatrick, E. L. 1985, ApJ, 299, 219

- Fitzpatrick, E. L. 1986, AJ, 92, 1068
- Franceschini, A., Silva, L. & Danese, L. 1997, ApJ, submitted (astro-ph/9707064)
- Giavalisco, M., Steidel, C., & Macchetto, D. 1996, ApJ, 470, 189
- Giovanelli, R., Haynes, M. P., Salzer, J. J., Wegner, G., da Costa, L. N. D., & Freudling, W. 1994, AJ, 107, 2036
- Gordon, K. D., Calzetti, D., & Witt, A. N. 1997, ApJ, 487, 625
- Guiderdoni, G., Hivon, E., Bouchet, F. R., & Maffei, B. 1997, MNRAS, in press (astro-ph/9710340)
- Heney, L. G., & Greenstein, J. L. 1941, ApJ, 93, 70
- Kauffmann, G. A. M., 1995, MNRAS, 274, 161
- Kylafis, N. D., & Bahcall, J. M. 1987, ApJ, 317, 637
- Kuchinski, L. E., Terndrup, D. M., Gordon, K. D. & Witt, A. N. 1998, AJ, 115, 1438
- Lacey, C. G., Guiderdoni, G., Rocca-Volmerange, B. & Silk, J. 1993, ApJ, 402, 15
- Madau, P., Ferguson, H. C., Dickinson, M. E., Giavalisco, M., Steidel, C. C. & Fruchter, A. 1996, MNRAS, 283, 1388
- Peletier, R. F. & Willner, S. P. 1992, AJ, 103, 1761
- Peletier, R. F., Valentijn, E. A., Moorwood, A. F. M., & Freudling, W. 1994, A&AS, 108, 621
- Pfenniger, D. & Combes, F. 1994, A&A, 285, 94
- Pozzetti, L., Madau, P., Zamorani, G., Ferguson, H. C., & Bruzual, G. A. 1998, MNRAS, in press
- Rowan-Robinson, M. *et al.* 1997, preprint (astro-ph/9707030)
- Silva, L., Granato, G. L., Bressan, A. & Danese, L. 1998, ApJ, in press (astro-ph/9806314)

- Smail, I., Ivison, R. J., & Blain, A. W. 1997, preprint (astro-ph/9708135)
- Xilouris, E. M., Kylafis, N. D., Papamastorakis, J., Paleologou, E. V., Haerendel, G. 1997, A&A, 325, 135
- Xilouris, E. M., Alton, P. B., Davies, J. I., Kylafis, N. D., Papamastorakis, J., Trewella, M. 1998, A&A, 331, 894
- Wise, M. W. & Silva, D. R. 1996, ApJ, 461, 155
- Witt, A.N., Thronson, H.A., & Capuano, J.M. 1992, ApJ, 393, 611
- White, S. D. M. & Frenk, C. S. 1991, ApJ, 379, 52

TABLE 1 - Model Properties

Model	Galaxy Type	η^a	Ext. Law	Dust Distrib.	ξ^b	Notes
S01_ME04	Spiral	0.1	Milky Way	Exponential	0.4	
S04_ME04	Spiral	0.4	Milky Way	Exponential	0.4	
S16_ME04	Spiral	1.6	Milky Way	Exponential	0.4	
S01_ME10	Spiral	0.1	Milky Way	Exponential	1.0	
S04_ME10	Spiral	0.4	Milky Way	Exponential	1.0	
S16_ME10	Spiral	1.6	Milky Way	Exponential	1.0	
S01_ME25	Spiral	0.1	Milky Way	Exponential	2.5	
S04_ME25	Spiral	0.4	Milky Way	Exponential	2.5	
S16_ME25	Spiral	1.6	Milky Way	Exponential	2.5	
S04_MD20	Spiral	1.6	Milky Way	Exponential	2.0	Rad. extended dust
S01_SE04	Spiral	0.1	SMC	Exponential	0.4	
S04_SE04	Spiral	0.4	SMC	Exponential	0.4	
S16_SE04	Spiral	1.6	SMC	Exponential	0.4	
S01_SE10	Spiral	0.1	SMC	Exponential	1.0	
S04_SE10	Spiral	0.4	SMC	Exponential	1.0	
S16_SE10	Spiral	1.6	SMC	Exponential	1.0	
S01_SE25	Spiral	0.1	SMC	Exponential	2.5	
S04_SE25	Spiral	0.4	SMC	Exponential	2.5	
S16_SE25	Spiral	1.6	SMC	Exponential	2.5	
S04_SD20	Spiral	1.6	SMC	Exponential	2.0	Rad. extended dust
E_ME	Elliptical	—	Milky Way	Exponential	$z_d = 50\text{pc}$	
E_SE	Elliptical	—	SMC	Exponential	$z_d = 50\text{pc}$	
E_MC	Elliptical	—	Milky Way	Constant	—	
E_SC	Elliptical	—	SMC	Constant	—	
E_MJ	Elliptical	—	Milky Way	Jaffe	—	
E_SJ	Elliptical	—	SMC	Jaffe	—	
E_MR	Elliptical	—	Milky Way	$1/r$	—	
E_SR	Elliptical	—	SMC	$1/r$	—	

^a $\eta = r_e/r_*$ is the ratio between the bulge effective radius and the disk stellar scale length; $r_* = 4$ kpc.

^b $\xi = z_d/z_*$ is the ratio between the dust and the stellar disk vertical scale height; $z_* = 0.35$ kpc.

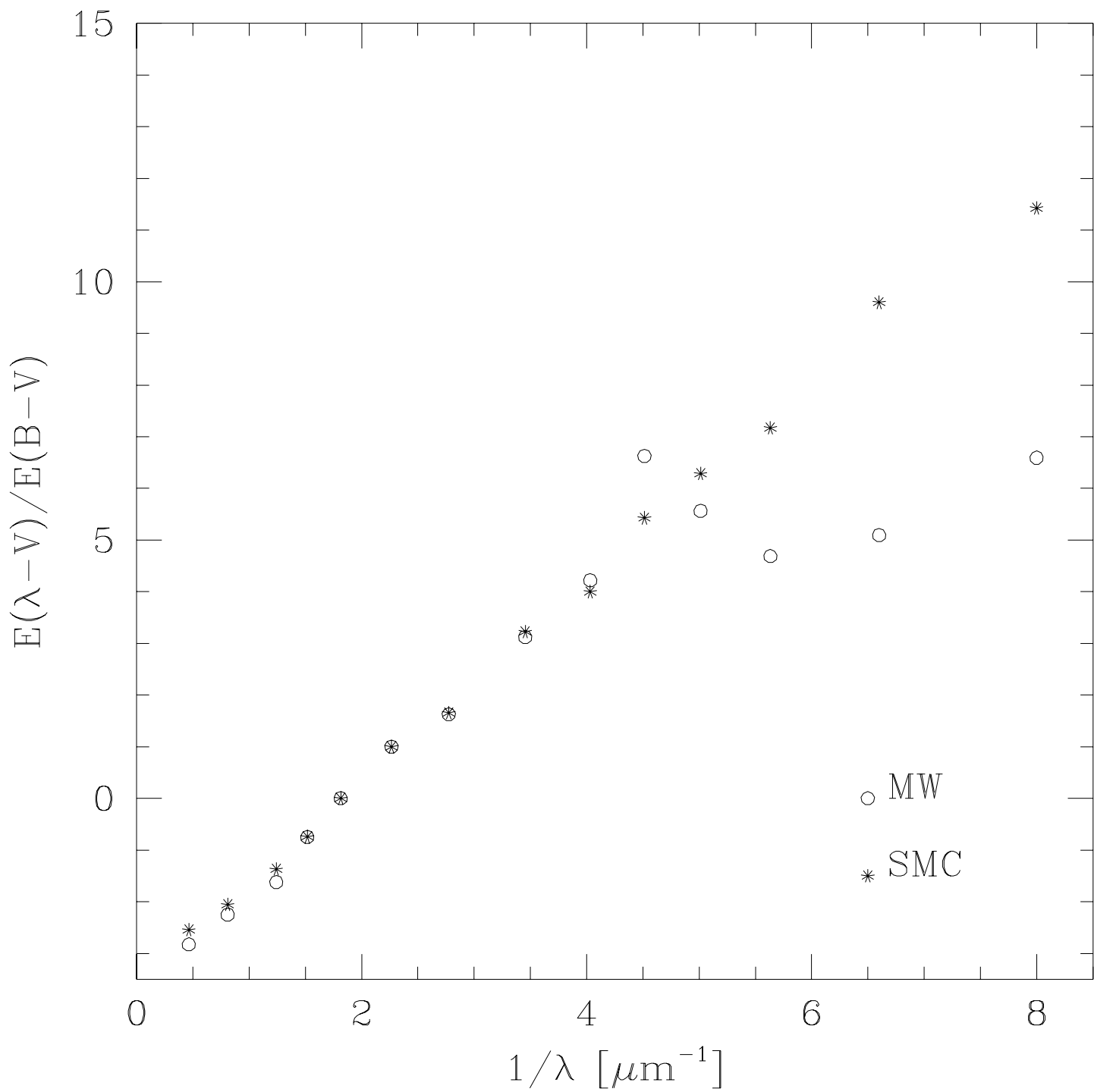


Fig. 1.— Adopted extinction curves for the Milky Way (open circles) and the Small Magellanic Cloud (stars).

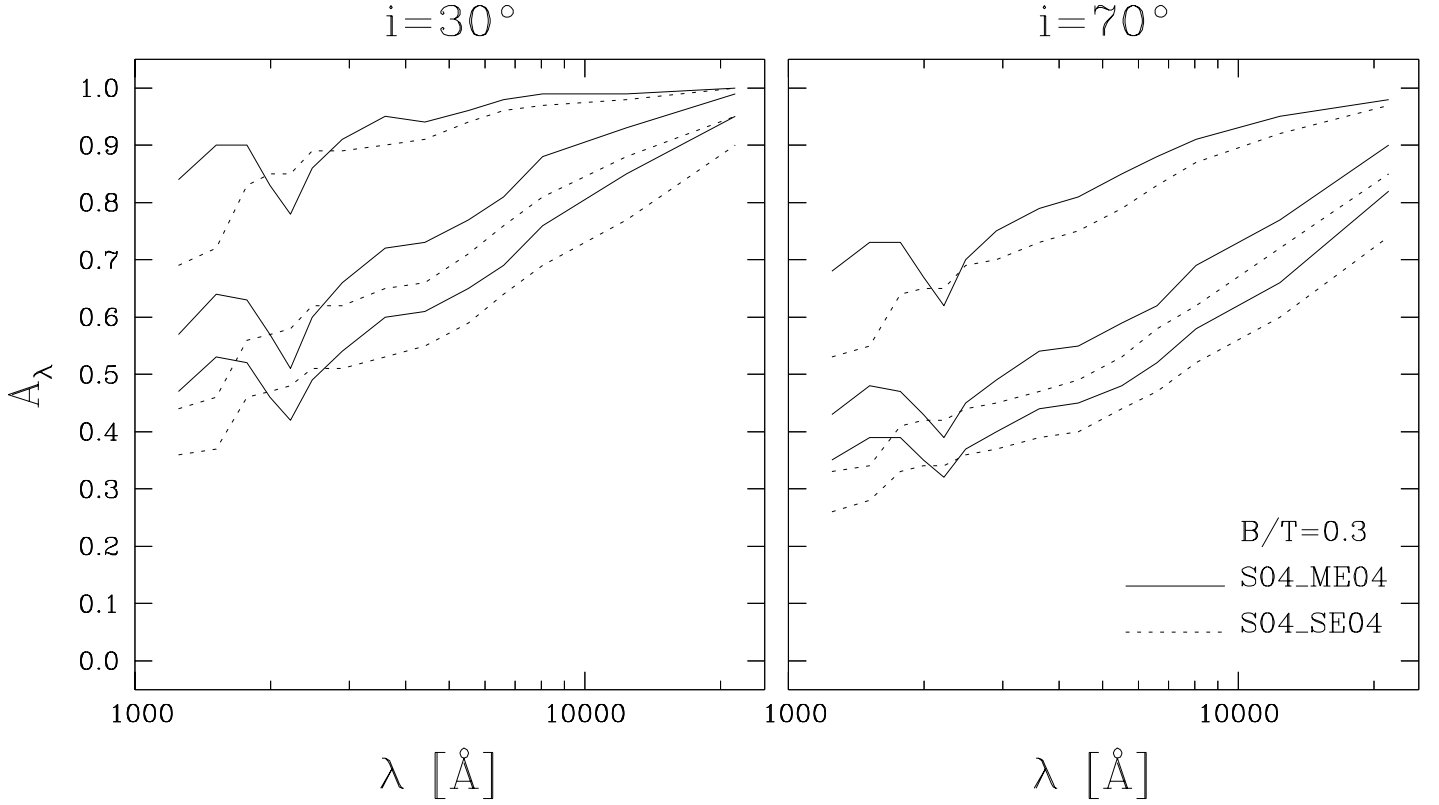


Fig. 2.— Attenuation curves for the model S04_ME04 (*solid* curves) and S04_SE04 (*dotted*) as a function of wavelength; model parameters are defined in Tab. 1. The curves are shown for bulge-to-total ratio $B/T=0.3$, two inclination angles $i = 30^\circ, 70^\circ$, and optical depths $\tau_V = 1, 5, 10$ from the uppermost to the lowermost curve in each panel.

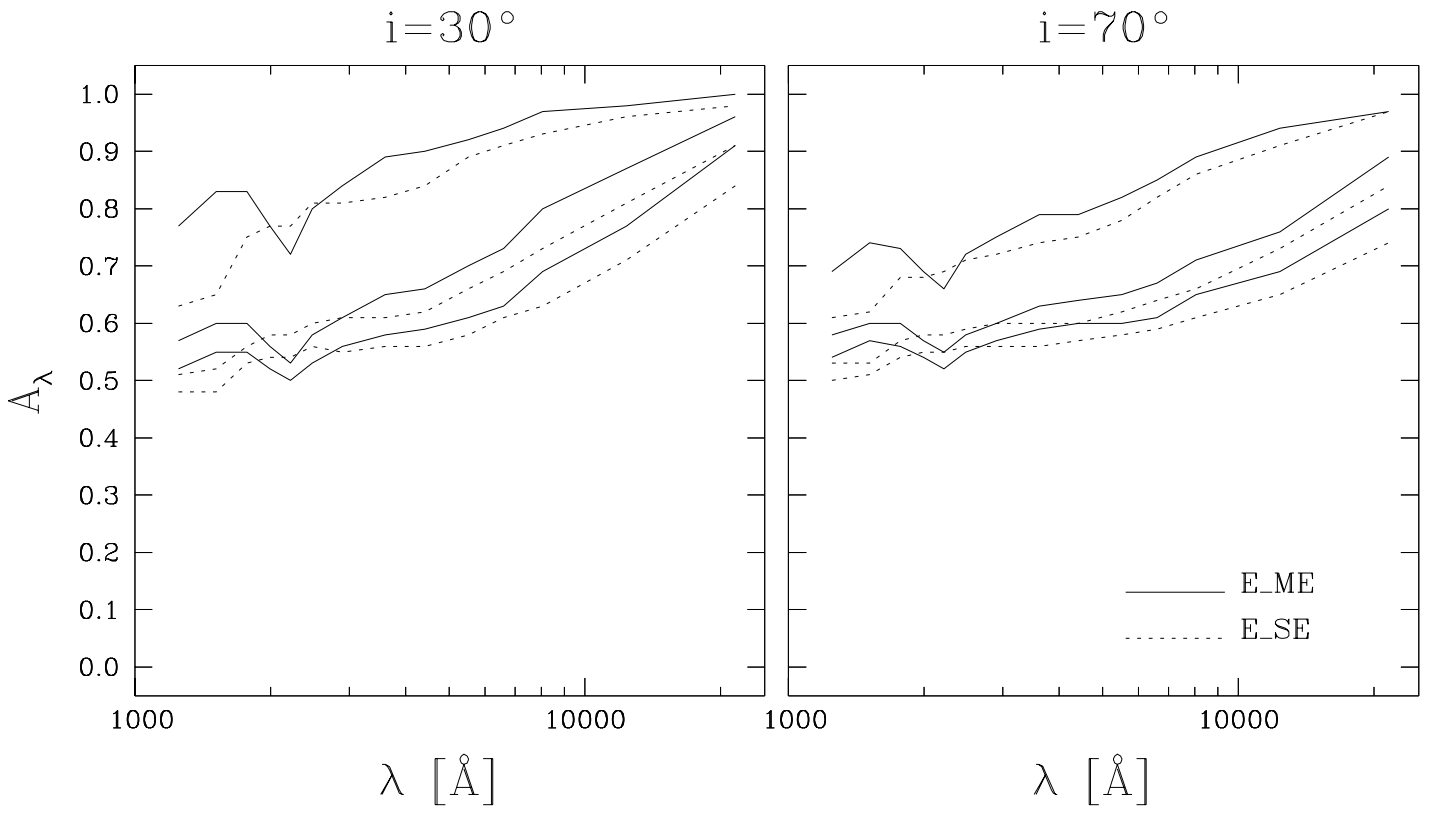


Fig. 3.— Same as Fig. 2 for the models E_ME and E_SE; model parameters are defined in Tab. 1.

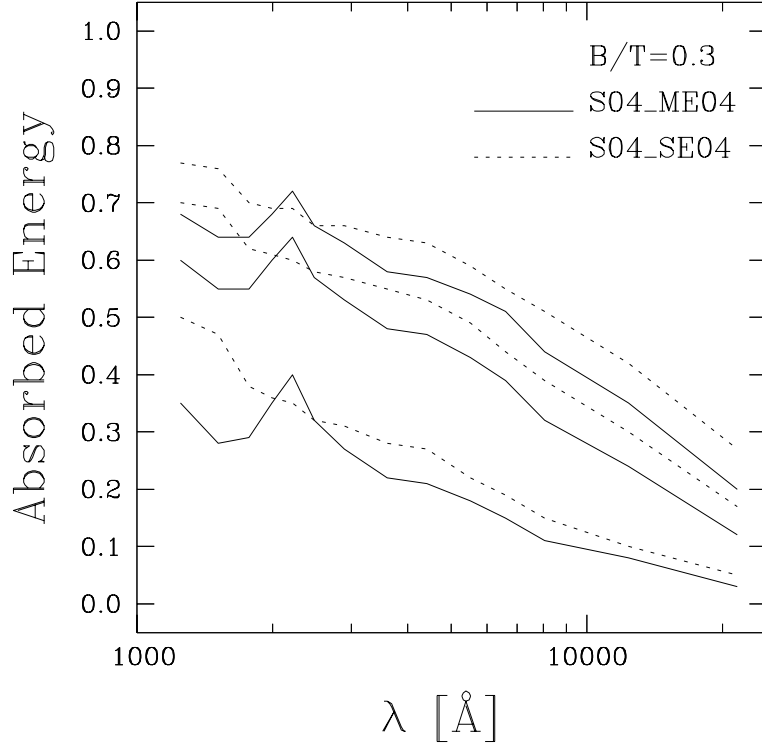


Fig. 4.— Fraction of the emitted energy absorbed by dust as a function of wavelength for the models S04_ME04 (*solid* curves) and S04_SE04 (*dotted*) as a function of wavelength; model parameters are defined in Tab. 1. The curves are shown for bulge-to-total ratio $B/T=0.3$ and optical depths $\tau_V = 1, 5, 10$ from the lowermost to the uppermost curve in each panel.

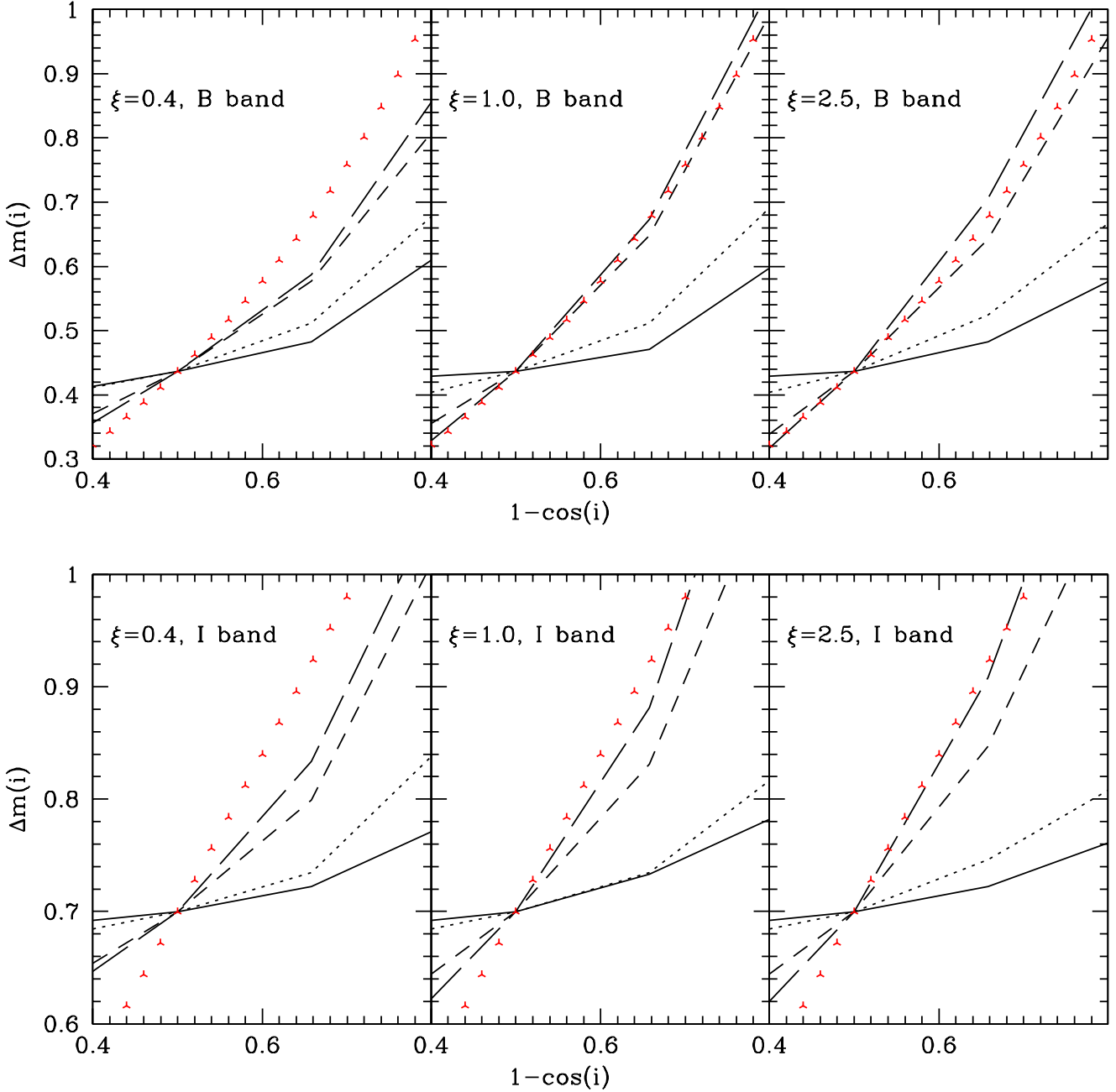


Fig. 5.— Dependence of the internal extinction correction Δm on $1 - \cos(i)$ for the B-band (upper three panels) and I-band (lower panels). Points are observational data from de Vaucouleurs *et al.* (1991) (B-band) and Bernstein *et al.* (1994) (I-band); note that the vertical offset of the data is arbitrary. Curves are from models S04_ME $_{xx}$ for B/T=0.1, where xx=04,10,25 (or $\xi = 0.4, 1.0, 2.5$);